



Influence of FRP confinement on bond behavior of corroded steel reinforcement

Christos G. Papakonstantinou^{a,*}, Perumalsamy N. Balaguru^b, Yubun Auyeung^c

^a University of Thessaly, Department of Civil Engineering, Pedion Areos, 38334 Volos, Greece

^b Rutgers, The State University of New Jersey, 623 Bowser rd, Piscataway, NJ 08854, United States

^c Axis Design Group, 744 Broad st, Newark, NJ 07102, United States

ARTICLE INFO

Article history:

Received 28 January 2010

Received in revised form 1 August 2010

Accepted 8 February 2011

Available online 23 February 2011

Keywords:

Composite

Concrete

Fiber reinforcement

Corrosion

Bond strength

Confinement

ABSTRACT

This study investigates the bond behavior of corroded reinforcing steel confined with carbon fiber reinforced polymer (CFRP). Corrosion of steel reinforcement in reinforced concrete structural elements could pose a significant problem that may result in loss of structural capacity and even failure. Very few studies have investigated the performance of the bond in corroded confined specimens. The conclusions from these studies suggest that the confinement prevents the reduction of bond strength even after considerable deterioration. Results reported in this paper provide quantitative information regarding the effectiveness of CFRP confinement. Bond tests were conducted on pull-out specimens with 10, 13, 19, and 25 mm [#3, #4, #6, and #8] diameter steel bars corroded to various levels and confined with CFRP. The primary independent variables investigated were: four bar sizes, various levels of corrosion and number of CFRP layers used for confinement. The results indicate that confinement can be effectively used to prevent the degradation of bond strength even at the highest levels of corrosion (12% mass loss) evaluated in this study. The loss of strength for unconfined specimens reached as high as 80%. As expected, confinement was more effective in bars with larger relative rib area. Confinement was also effective in maintaining the ductility.

© 2011 Elsevier Ltd. All rights reserved.

1. Introduction

Corrosion of reinforcing steel in reinforced concrete is a significant problem throughout the world. It is estimated that more than a hundred billion dollars is needed for the rehabilitation of existing transportation related structures in the US. More than half of these structures are made of reinforced concrete, and their main deficiencies are associated with reinforcement corrosion. The problem is more acute in cold climates, where deicing chemicals are being used. Corrosion of reinforcement results in reduction of cross sectional area and loss of bond strength. When loss of diameter exceeds 2%, cross sectional area reduction could be quite substantial leading to significant reduction bond strength [1]. In addition, information on bond behavior is necessary to estimate the capacity of structural elements with corroded reinforcement. A number of studies have examined the performance of the bond between concrete and corroded reinforcement [1–9]. The major variables evaluated were: influence of corrosion level on bond strength, slip, ductility, bar size and type, cover, and characteristics of concrete including concrete containing various chemical and mineral admixtures (latex, methylcellulose, silica fume) [2]. The major findings from these studies are: bond strength increases for small amount of corrosion (section loss lower than 0.5%) but

decreases at higher levels of corrosion (section loss higher than 4%) [1,8], admixtures in concrete can improve the bond [2], surface characteristics of corroded bars influence their bond behavior [3] and corrosion causes significant reduction in ductility [9]. However, these studies did not include the effect of confinement, and hence, can only be used for modeling of tensile reinforcement without confinement (stirrups, transverse reinforcement, etc.). Typical examples are one-way slabs and bridge decks. Since the problems of corrosion are not limited to these types of structures, a better understanding of the bond behavior of confined corroded reinforcement is needed.

A relatively limited amount of beam and column test results [9–15] is available in the literature regarding the corrosion of reinforcement with confinement. Due to the significant amount of work needed for construction, instrumentation, and testing of large beam and column specimens, only small-scale beam tests with mostly small diameter tensile reinforcements (12 mm [#4] or less) were studied in these programs. The first study that introduced the idea of using fiber reinforced polymer sheets for confinement was published by Kono et al. [16], and focused on the effect of carbon fiber reinforced polymers (CFRP) sheets on the bond of non-corroded steel reinforcing bars to concrete. There are many advantages in using FRPs as opposed to embedding stirrups in the bond specimens. First, the FRP system eliminates any interference that stirrups might cause during the corrosion process. The confinement provided by carbon fibers is similar to the effects of stirrups

* Corresponding author. Tel.: +30 6984440253.

E-mail address: cpapak@gmail.com (C.G. Papakonstantinou).

in a sense that the level of confinement is a function of the bond stress exerted on the reinforcing bar. Also, the confining forces can be easily and accurately measured along the length of the specimen. This allows for the accurate estimation of confinement stresses along the length of the embedded reinforcing bar.

An investigation by Soudki and Sherwood [14] is the only study available in the literature that provides insight to the effects of concrete cover on the bond properties of corroded reinforcing bars. It is also the only study in which CFRP sheets were used for confinement of pull-out specimens. In their study the research focused on one bar size of 10 mm [#3]. Craig and Soudki [17] also reported the results of a study on reinforced concrete beams with corroded reinforcement strengthened with CFRP. Their findings suggest that confinement resisted the expansion due to cracking and maintained the interlock between the steel and concrete. Fang et al. [10] reported on a limited number of experiments on pull-out specimens confined using transverse reinforcement. Although their findings indicate that the role of confinement is important in cases of low corrosion (less than 4%), the effect cannot be related to bar diameter since only one bar diameter (20 mm [#6]) was used in the study. In all these studies bar diameter was not an experimental variable. Since, it is well documented that rib geometry with respect to bar sizes plays an important role on the bond behavior of corroded reinforcement [18,19], more information is needed on the effect of bar diameter on the performance of confined corroded reinforced concrete elements.

The objective of this investigation is to study the effects that confinement, corrosion level and reinforcement sizes have on the bond behavior of confined reinforcing steel using pull-out tests. The following were the major tasks:

1. Obtain bond strength and bond–slip behavior on 10 mm [#3], 13 mm [#4], 19 mm [#6], and 25 mm [#8] diameter reinforcing bars with different levels of confinement and corrosion.
2. Determine the effects of the amount of confining reinforcement on the bond behavior.
3. Compare bond behaviors between non-confined and confined pull-out specimens.

2. Specimen details and preparation

A series of 48 pull-out specimens were fabricated and tested. Confinement was introduced using carbon fiber reinforced polymer (CFRP) sheets wrapped around the pull-out specimens. The main parameters examined were the diameter of the reinforcement,

the magnitude of corrosion and number of CFRP sheets used for confinement. Pull-out specimens conforming to the Danish Standards DS 2082 [20] were fabricated with 10 mm [#3], 13 mm [#4], 19 mm [#6], and 25 mm [#8] diameter reinforcing bars (see Fig. 1). Twelve specimens were allocated for each reinforcement size, with three concrete cylinders for each bond specimen for Young's modulus and compressive strength tests and five cylinders from each batch of concrete mix for splitting tensile tests. A new batch of concrete mix with the same mix design was used for each bar size.

The molds were constructed using epoxy-coated plywood. Because the pullout test was conducted by applying tensile forces to long and short bars, they were aligned precisely in order to obtain accurate results. In addition, both bars had to be placed concentrically at the center of the cross section. The precise placement of bars was achieved using two 100 mm [4 in.] long pipes with an opening of 38 mm [1.5 in.]. These pipes were attached to the two end boards of the molds, while two sets of three screws were threaded into the pipe to align and grip the ends of the deformed bars. This arrangement ensured the correct alignment of both bars. The embedment length of the short bars was calculated as a function of the bar diameter, using equation 12-1 in ACI 318-05 [21], and is shown in Fig. 1. The concrete mix consisted of ASTM Type I cement, concrete, sand, 9 mm [0.35 in.] maximum size coarse aggregate, and tap water. The admixtures for the concrete were 3% by cement weight of calcium chloride (curing accelerator) and 0.1% by cement weight of air entrainment admixture. The cement, fine and coarse aggregate ratio was 1:1.7:2.0 and the water–cement ratio was 0.48. An average compressive strength of 35 MPa [5000 psi] was obtained for this concrete mix proportion.

A carbon fiber reinforcing system was chosen as the method to provide confinement. This system consists of unidirectional carbon fiber sheets, a two-part epoxy primer and a two-part epoxy matrix. It should be noted that the application of the CFRP was done after the specimens were corroded. The design properties of the CFRP system used in this study are provided in Table 1.

Carbon plates were fabricated using the resin provided by the manufacturer. After sufficient curing of the matrix, two layers of glass fabric in the $\pm 45^\circ$ direction of the carbon were laid out on each gripping surface of the plate and attached using the epoxy matrix. The composite plates were cut into coupons for strength and Young's modulus testing. Twenty-three coupons were tested, 12 of which were coupons with one layer of carbon with widths ranging from 17.5 mm to 28.8 mm [0.69–1.13 in.], and 11 of which

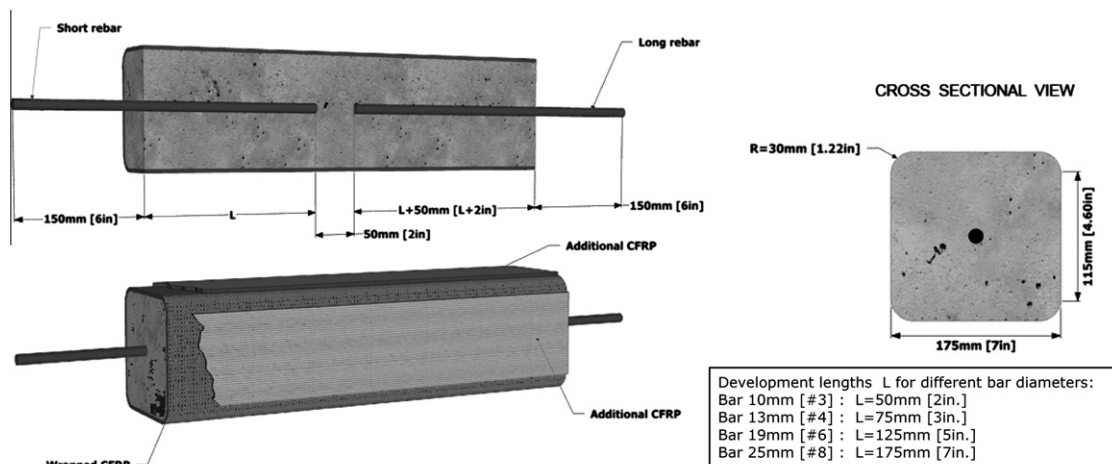


Fig. 1. Details of bond specimen confined by carbon fiber sheets.

Table 1
Properties of high strength carbon fibers.

	Provided by the manufacturer	Uniaxial tension coupon testing
Weight of fiber (g/cm ²) [lb/ft ²]	200 [409.3]	N/A
Gravity of fiber (g/cm ³) [lb/ft ³]	1.82 [113.6]	N/A
Design thickness (mm) [in.]	0.11 [0.0043]	N/A
Standard execution thickness (mm) [in.]	0.45 [0.0177]	N/A
Tensile strength (kgf/cmw) [kip/inw]	390 [2.18]	436.2 [2.48]
Tensile design strength (MPa) [ksi]	3480 [505]	3892 [564]
Tensile modulus (kgf/cmw) [lbf/inw]	25850 [144.5]	29609 [165.5]
Tensile design modulus (MPa) [ksi]	230460 [33425]	263820 [38290]
Deformation ratio at failure (%)	1.5	1.47

were coupons with two layers of carbon with widths ranging from 18.6 mm to 27.5 mm [0.73–1.08 in.]. For the coupons with one layer of carbon, strain readings were taken every 445 N [100 lb] and for the coupons with two layer of carbon, strain readings were taken every 890 N [200 lb]. A summary of experimental tensile strength tensile modulus, and strain at failure are also presented in Table 1.

For the application of each wrapped carbon fiber sheet, an overlap length of 100 mm [4 in.] was chosen. The wrapping was applied for the entire length of the concrete prism. For specimens with two layers of wrapping, each layer was applied separately rather than a continuous wrapping. In addition to the wrapping of the specimen, strips of carbon sheet were also applied to the bond specimens to prevent premature tensile failure of concrete, as shown in Fig. 1. The widths of the carbon strip are provided in Table 2. The strips were divided into two equal parts and were applied on the two opposite sides of the bond specimen.

The details of the bond specimen with carbon fibers are shown in Fig. 1. Before the application of the CFRP, 3 mm [0.1 in.] of surface concrete were removed by means of a diamond-grinding wheel, exposing the stronger concrete, thus ensuring adequate bond of carbon fiber sheets. The corners of the specimens were then ground to a minimum radius of 30 mm [1.18 in.] to allow proper stress transfer of the composite around the corners of the specimens. This was the main modification of the specimens specified by the Danish Standards [20]. All surfaces on the specimens were then sand blasted to remove any loose particles. Prior to application of the carbon composite, the specimens were allowed to dry for 3 days.

Depending on the surface condition, two to three layers of primer were applied to the specimens and allowed to dry for 9 h. After proper curing of the primer, the matrix was brushed onto the concrete surfaces, and the carbon fiber sheet was placed onto the fresh matrix. The unidirectional fabric was positioned so that the direction of the fibers was perpendicular to the direction of the steel bars. A saturation roller was used to remove air pockets in the sheet. An additional coat of matrix was then applied on top of the carbon sheet, and a rubber scoop was used to rub the matrix into the carbon fibers. The specimen was then allowed to cure for one to 2 weeks, depending on the temperature at the time of application.

Table 2
Width of carbon sheet for additional tensile reinforcement.

Reinforcement diameter (mm) [bar #]	Width of carbon sheet for additional tensile reinforcement (cm) [in.]
10 [#3]	10 [3.93]
13 [#4]	13 [5.12]
19 [#6]	17 [6.7]
25 [#8]	41 [16.1]

The electrolyte corrosion technique, in which a direct current is passed from the reinforcement to the four copper plates attached to the sides of the specimen, was chosen as the method to induce corrosion. The copper plates; which serve as cathodic sites, consume the excess electrons provided by the power supply. The power supply that was used to induce corrosion had a maximum output of 24 VDC and 12 amps. The positive terminal was connected to the short deformed bar and the negative terminal was connected to the copper plates (see Fig. 2). To prevent the corrosion of exposed bar at the junction of concrete, a rubber coating, acting as an insulator, was applied to the bar and the top surface of the concrete. Uniform corrosion along the length of the embedded reinforcing steel was achieved using this rubber coating. After the power supply was turned on, the current flowing through the system was recorded at 1-min intervals using a computer-controlled data acquisition system. An average current density of 3 mA/cm² was maintained for each corrosion process. The amount of corrosion is a function of current and time. The mass loss of reinforcing steel due to corrosion can be estimated by the following equation, which is based on Faraday's law:

$$M_t = \frac{t \times \bar{I} \times M}{z \times F} \quad (1)$$

where t is the duration of exposure (s), \bar{I} is the average current (amperes), F (Faraday's constant) is taken equal to 96,500 As, z is the ionic charge (2 for Fe), and M is the atomic weight of the metal (56 g for steel). The quantity of applied charge for any electrolysis is given by the product of applied current and the duration of current application. For the corrosion process, for each mole of iron oxidized, 2 mol of electrons are given out, consuming a charge of $2 \times 96,500$ C. The mass loss is then calculated by multiplying the

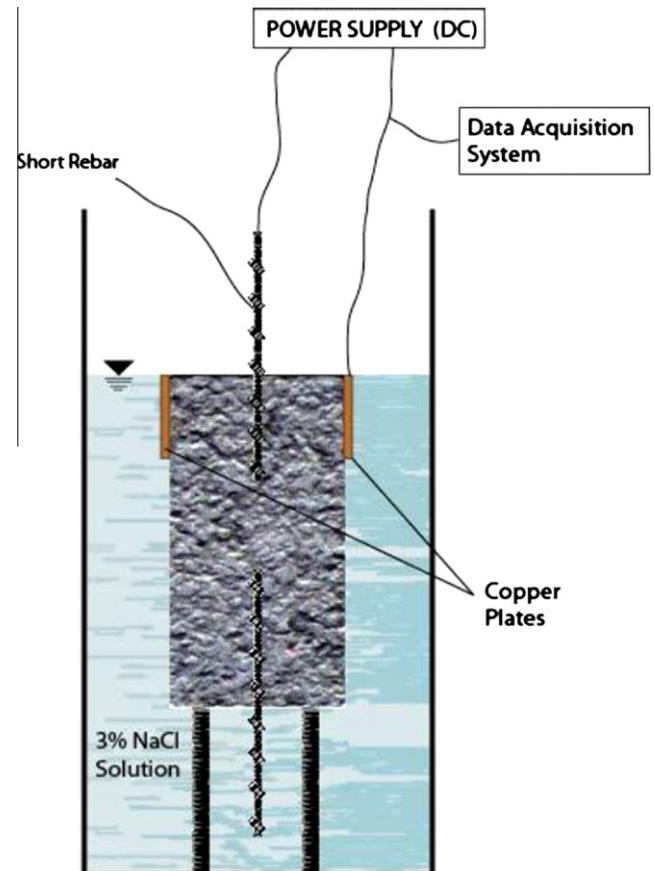


Fig. 2. Setup for inducing accelerated corrosion.

applied charge by the molar mass (55.847 g/mol for iron) and dividing by the charge needed per mole. This technique was successfully adopted by several researchers to induce corrosion in reinforced concrete elements [20].

A series of pull-out tests on unconfined specimens were conducted to develop relationships between bond strength and corrosion level. The unconfined specimens were identical to the confined specimens, except from the application of the CFRP. The relationships developed were specific to a particular bar size. A typical graph, for 13 mm [#4] bars, is shown in Fig. 3. In this graph the curve, which was obtained from eleven tests conducted on unconfined specimens with different corrosion levels (dots in the graph), illustrates the relationship between the bond strength and corrosion level in terms of percentage mass loss. Five different levels of bond strength, designated as μ_o , μ_a , μ_b , μ_c , μ_{res} were identified as shown in Fig. 3. μ_o designates the bond strength at 0% corrosion and μ_{res} the residual bond strength. The remaining three values μ_a , μ_b , μ_c were obtained by dividing the difference $\mu_o - \mu_{res}$ by 4. The target was to determine values of corrosion (A–D) that would correspond to equal reductions in bond strength (Fig. 3). Since the focus of the current investigation was on the repair and rehabilitation of corroded reinforced concrete elements, the region above the bond strength μ_o was not considered. For each of the four levels of corrosion and for each bar size, three specimens were fabricated. The four corrosion levels A–D for 10, 13, 19, and 25 mm [#3, #4, #6, and #8 bars] diameter bars are presented in Table 3.

In each group, a specimen was used as control without the addition of carbon fiber confinement; one specimen was wrapped with one CFRP layer, and a third specimen was wrapped with two layers of carbon fiber sheets. This way we were able to simulate two levels of confinement. A total of 48 specimens were tested for this experimental study. For all specimens wrapped with carbon fiber sheets, strips of carbon fiber sheets were also attached along the length of the specimen to prevent tensile failure of concrete (see Fig. 1).

3. Testing procedure

A schematic diagram of the pullout specimen is shown in Fig. 4. The pullout load was applied using friction tension grips. The tests

Table 3
Corrosion levels for different bar sizes.

Reinforcement diameter (mm) [bar #]	Corrosion level	Mass loss (%)
10 [#3]	A	3.98
10 [#3]	B	4.51
10 [#3]	C	5.25
10 [#3]	D	7.99
13 [#4]	A	1.47
13 [#4]	B	1.87
13 [#4]	C	2.47
13 [#4]	D	5.80
19 [#6]	A	2.44
19 [#6]	B	3.39
19 [#6]	C	4.94
19 [#6]	D	7.92
25 [#8]	A	0.34
25 [#8]	B	0.58
25 [#8]	C	0.82
25 [#8]	D	2.01

were conducted using a 500 kN [110 kip] electromechanical testing frame. The bond–slip behavior was recorded using two dial gauges mounted on opposite sides of the bond specimen (Fig. 4). Readings were recorded every 90 N [20 lb] for 10 and 13 mm [#3 and #4] bars and every 220 N [50 lb] for 19 and 25 mm [#6 and #8] bars. To measure strain and stress on the CFRP demountable mechanical strain gauges (DEMEC) were used. Conical locating points were placed as shown in Fig. 4. The conical locating points, were made out of stainless steel, and had a diameter of 7 mm [0.27 in.] and a thickness of 4 mm [0.16 in.]. Two conical locating points were used for each location and the distance between them was measured by a special attachment mounted on a digital caliper. The DEMEC enabled measurements of lateral strain (lateral to the direction of the steel bars) of the carbon composites along the length of the embedded reinforcing bar. From the strain measurements, a distribution of confining force can be calculated. For specimens with 10 and 13 mm [#3 and #4] diameter reinforcement, each set of DEMEC were placed at 13 mm [0.5 in.] intervals and for specimens with 19 and 25 mm [#6 and #8] diameter

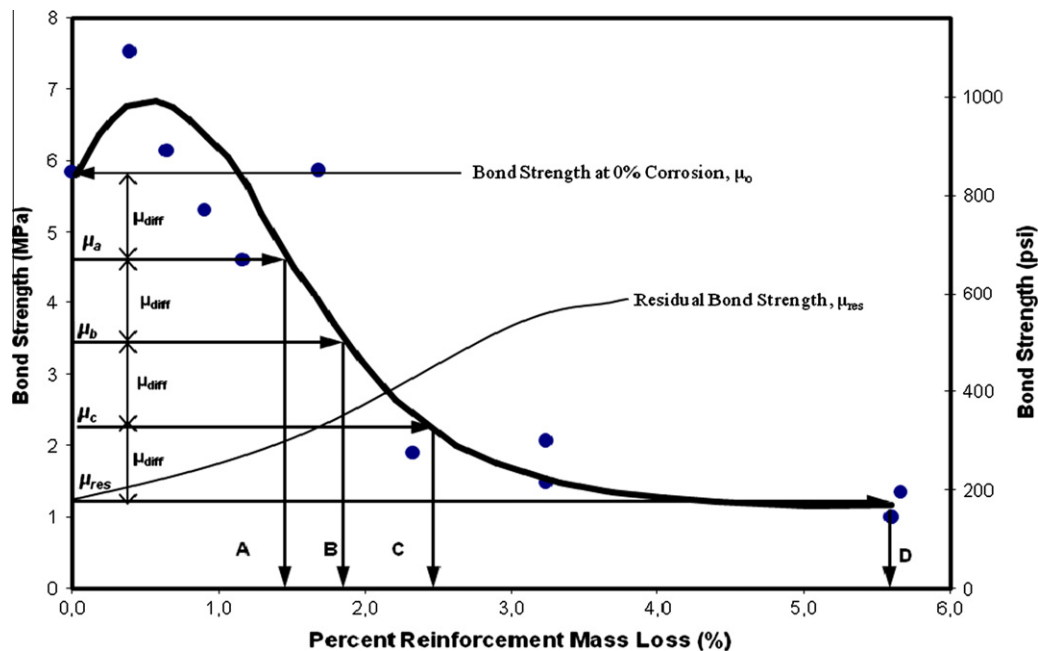


Fig. 3. Typical levels of corrosion (% mass loss) for non-confined specimens with 13 mm [#4] diameter bars.

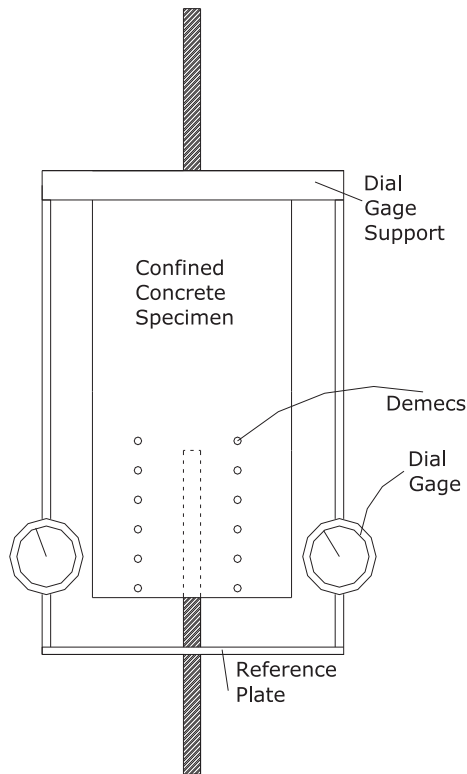


Fig. 4. Details of confined DS2082 bond specimen.

reinforcement, each set of DEMEC gauges were placed at 25 mm [1 in.] intervals. From the initial testing of the DEMEC measurements, the resolution of strain reading was determined to be $\pm 2 \times 10^{-4}$. For all bond specimens, readings were recorded every 4.4 kN [1 kip].

After the completion of the pullout test, the corroded bars were removed from the specimens and cleaned by wire-brushing to remove the corrosion product. The cleaned bar was weighted and the total percentage loss was computed. Mass losses were obtained along the length of the bar to ascertain the uniformity of measured corrosion. The comparison of mass change between control and corroded bar provided the mass loss for every 6 mm [0.25 in.]. The mass losses were added to obtain the cumulative mass loss presented in the results section.

4. Experimental results and discussion

To improve clarity, test results and their analysis are presented in the following four sections:

- Stress distribution in the confining carbon composite.
- Effect of confinement on the bond strength of corroded reinforcement.
- Effect of confinement on the slip at failure at different corrosion levels.
- Effect of confinement on the load-slip behavior at various corrosion levels.

4.1. Distribution of tensile stress in the confining carbon composite

The strain in the carbon composite was measured and recorded during pull-out bond testing. Using the mechanical properties obtained from carbon coupon tests (shown in Table 1), the tensile stress distributions of the carbon composite (along the direction of the fibers and lateral to the direction of the bar) corresponding

to 95% of the ultimate pullout load are shown in Fig. 5. In parts (a) and (b) of Fig. 5 the curves present the distribution of the CFRP stresses along the length of specimens exposed at low corrosion level (level A), while curves (c) and (d) refer to specimens with high corrosion levels (level D). In order to investigate the effects of the bar size and stress level on the stress distribution the values for the distance from free end were normalized with respect to the embedment length. The distance from free end shown is the distance along the reinforcement's axis from the end of the concrete prism for which the corroded bar was embedded (maximum distances varied from 50 to 175 mm [2–7 in.], based on the embedment length L value shown in Fig. 1). It should be noted, that CFRP stress distribution varies very little along the length of the embedded reinforcement for loads close to 50% of the ultimate pullout load. At this low pullout load the stresses did not exceed 75 MPa [10,875 psi]. No apparent trends with respect to bar sizes and corrosion levels were observed and the magnitude of the recorded tensile stress was very low, signifying that the concrete is resisting most of the pullout force.

For the stress distribution at 95% of the ultimate pullout load, however, the tensile stress in the carbon increases linearly toward the free end of the concrete prism, meaning that sufficient damage was done to the surrounding concrete and the confining reinforcement is resisting the majority of the bursting stress caused by the reinforcement.

The observed specimen performance could be explained using the relative rib area, as described by Soretz and Holzenbein [18] and Darwin and Graham [19], given by:

$$R_r = \frac{A_r}{P \times S_r} \quad (2)$$

where R is the relative rib area, A is the projected rib area normal to bar axis, P is the nominal bar perimeter, and S_r is the center-to-center rib spacing. The relative rib area for the 10, 13, 19, and 25 mm [#3, #4, #6, and #8] reinforcement used in this study is 0.042, 0.037, 0.070, and 0.080, respectively. So, essentially there are two groups based on the relative rib area. One that includes 10 and 13 mm [#3, #4] bars with small rib areas 0.042 and 0.037, and one that includes 19 and 25 mm [#6, #8] with larger relative rib areas of 0.07 and 0.08 respectively. As indicated by Darwin and Graham [19], for confined specimens, increase in relative rib area corresponds to increase in the magnitude of the tensile stress of the confining reinforcement. This conclusion is validated in Fig. 5, as for 10 and 13 mm [#3, #4] diameter bars, with small relative rib areas, there seems to be no apparent trend in the tensile stresses of the carbon composite with respect to the amount of corrosion or even number of CFRP layers. On the contrary, the recorded CFRP stresses at the free end of the specimen seem to be significantly higher for larger diameter bars (19 and 25 mm [#6, #8]) with larger relative rib areas. It also seems that lower levels of corrosion (level A) result in an increase of CFRP stresses compared to higher levels of corrosion (level D), suggesting that corrosion results in a reduction of relative rib areas. Thus, the bursting stress that the confining reinforcement is required to resist is reduced and hence the confining jacket is stresses less. It is also evident from the graph that the addition of a second CFRP layer reduces significantly the stresses exerted on the CFRP when large size bars are used.

4.2. Effects of confinement on the bond strength of corroded reinforcing steel

As mentioned earlier, bond-slip behavior was obtained for 48 specimens with reinforcement diameters of 10, 13, 19, and 25 mm [#3, #4, #6, and #8]. Twelve specimens were tested for each bar size, 1/3 of which were without carbon confinement,

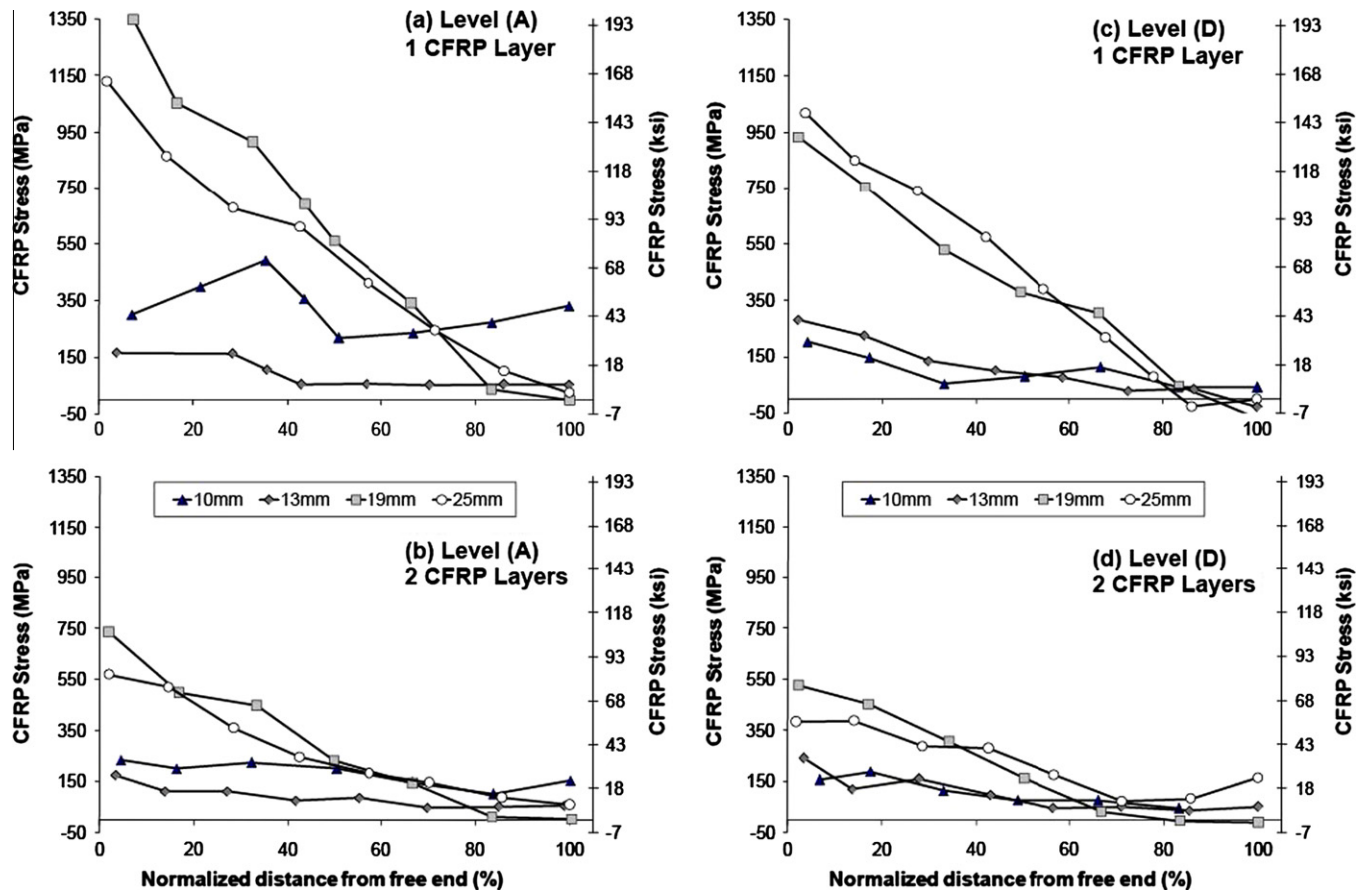


Fig. 5. Distribution of CFRP stresses (lateral to pullout load) corresponding to 95% of ultimate pullout load, for low and high corrosion levels [levels A (a and b) and D (c and d)] and specimens confined using one and two layers of CFRP.

1/3 of which were reinforced with one layer of carbon confinement, and the other 1/3 of which were reinforced with two layers of carbon confinement.

Detailed experimental results containing average bond strength, maximum pullout load, slip at 90% of failure pullout load, and percentage mass loss are shown in Table 4. Average bond strength, μ_{ave} , was calculated based on the following equation:

$$\mu_{ave} = \frac{P_{max}}{\pi \cdot d_b \cdot l} \quad (3)$$

where P_{max} is the maximum pullout load, d_b is the bar diameter, and l is the embedded length of the shorter reinforcing bar.

The corrosion levels, average bond strength (hereafter referred to as “bond strength”), and the number of layers of carbon to confine the bond specimens for 10, 13, 19, and 25 mm [#3, #4, #6, #8] bond specimens are presented in Table 5. The increase of bond strength is significantly higher for 19 and 25 mm [#6, #8] diameter bars compared to the two bars with smaller diameters. Also it can be noticed that the addition of the second CFRP layer results in an average increase of 30–40% regardless of the bar size for 10, 13, and 19 mm [#3, #4, #6] bars, while the increase was significantly higher for 25 mm [#8] bars. The relationships between bond strength and corrosion expressed in percent mass loss are shown in Fig. 6 for reinforcement diameters of 10, 13, 19, and 25 mm [#3, #4, #6, #8]. As mentioned previously, four corrosion levels (A–D) were considered, and since the actual amount of corrosion deviates from the theoretical amount of corrosion, the corrosion level is expressed in terms of percentage mass loss. The corrosion levels were obtained from the bond strength graph for unconfined specimens and therefore in some

cases the corresponding mass loss percentages for different levels may seem very close. For an easier examination of the results the data points in the graph are grouped in terms of reinforcement size (grayscale) and amount of confinement (shape). In Fig. 6 it can be seen that the effect of confinement increases as the corrosion level increases. This was observed for all bar sizes with the exception of one set of data from the 25 mm [#8] bond specimens. Also, it should be noted that the effect of confinement also becomes more noticeable as the diameter of the reinforcing bars increase. This could be explained by the increase in the rib height associated with the increase in reinforcement diameter, which increases the bearing stress of the reinforcement on the concrete and hence, increasing the effect of the confining reinforcement. In addition to the specimens being considered in this part of the research program, specimens with virtually no corrosion are also presented in the figure. It can be noted that the degradation of bond strength as the amount of corrosion increases is very small for the confined specimens (unlike non-confined specimens). It is characteristic that the bond strength of confined specimens with one layer of CFRP is approximately equal to the bond strength of unconfined specimens with no corrosion. For specimens with two layers of carbon, when compared to specimens with one layer of carbon, a slight increase in the bond strength was observed for all reinforcement sizes. Although non-corroded confined specimens were not tested for comparison, the increasing corrosion up to 12% mass loss did not seem to affect the bond strength. Therefore, it is clear that the confined specimens did not suffer from bond degradation due to increasing corrosion. This finding agrees with findings from previous experimental studies [10,22].

Table 4
Slip and bond strength test results.

Bar diameter (mm) [bar #]	Carbon layers	Bond strength (MPa) [ksi]	Maximum pullout load (N) [lb]	Slip at 90% of failure pullout load (mm) [in.]	% Mass loss (corrosion level)	
10 [#3]	0	5.9 [856]	9266 [2083]	0.088 [0.0035]	4.92 (A)	
	1	7.53 [1091]	11826 [2658]	0.135 [0.0053]	5.27 (A)	
	2	9.09 [1317]	14276 [3209]	0.175 [0.007]	4.92 (A)	
	0	4.74 [687]	7444 [1673]	0.058 [0.002]	5.99 (B)	
	1	9.49 [1375]	14904 [3350]	0.16 [0.006]	6.34 (B)	
	2	10.00 [1450]	15705 [3530]	0.18 [0.007]	6.86 (B)	
	0	3.89 [563]	6109 [1373]	0.065 [0.003]	6.68 (C)	
	1	8.99 [1303]	14119 [3174]	0.16 [0.006]	7.38 (C)	
	2	9.93 [1439]	15595 [3506]	0.21 [0.008]	7.38 (C)	
	0	1.83 [264]	2874 [646]	0.04 [0.002]	11.96 (D)	
	1	8.49 [1231]	13334 [2997]	0.17 [0.007]	10.55 (D)	
	2	9.36 [1357]	14700 [3305]	0.17 [0.007]	10.55 (D)	
	13 [#4]	0	5.49 [796]	16813 [3780]	0.11 [0.004]	2.50 (A)
		1	8.49 [1230]	26000 [5845]	0.16 [0.006]	2.39 (A)
2		8.87 [1285]	27164 [6107]	0.17 [0.007]	2.39 (A)	
0		5.26 [762]	16109 [3621]	0.10 [0.004]	3.17 (B)	
1		7.72 [1119]	23642 [5315]	0.15 [0.006]	3.04 (B)	
2		8.79 [1274]	26919 [6051]	0.20 [0.008]	3.17 (B)	
0		4.70 [681]	14394 [3236]	0.08 [0.003]	3.82 (C)	
1		8.06 [1168]	24684 [5549]	0.19 [0.007]	3.17 (C)	
2		8.70 [1261]	26644 [5989]	0.18 [0.007]	3.71 (C)	
0		1.77 [256]	5421 [1219]	0.05 [0.002]	6.61 (D)	
1		7.41 [1075]	22693 [5101]	0.18 [0.007]	7.92 (D)	
2		8.29 [1202]	25388 [5707]	0.20 [0.008]	6.86 (D)	
19 [#6]		0	3.11 [451]	23200 [5215]	0.08 [0.003]	4.18 (A)
		1	7.58 [1099]	56546 [12712]	0.85 [0.03]	4.14 (A)
	2	8.79 [1274]	65572 [14741]	0.83 [0.033]	4.06 (A)	
	0	1.97 [285]	14696 [3304]	0.06 [0.002]	6.16 (B)	
	1	6.67 [968]	49757 [11185]	0.65 [0.026]	5.68 (B)	
	2	9.26 [1343]	69078 [15529]	1.06 [0.042]	5.29 (B)	
	0	1.39 [201]	10369 [2331]	0.05 [0.002]	8.40 (C)	
	1	6.76 [979]	50429 [11336]	0.55 [0.02]	7.59 (C)	
	2	8.10 [1174]	60425 [13584]	0.71 [0.028]	7.71 (C)	
	0	0.56 [81]	4148 [932]	0.04 [0.002]	11.77 (D)	
	1	6.52 [945]	48638 [10934]	0.67 [0.027]	11.53 (D)	
	2	8.24 [1195]	61469 [13818]	0.74 [0.029]	8.40 (D)	
	25 [#8]	0	4.12 [597]	56617 [12727]	0.10 [0.004]	0.88 (A)
		1	5.34 [774]	73382 [16496]	1.57 [0.06]	0.78 (A)
2		5.80 [840]	79703 [17917]	1.29 [0.05]	0.94 (A)	
0		0.60 [87]	8245 [1854]	0.03 [0.001]	1.43 (B)	
1		5.65 [819]	77642 [17454]	1.55 [0.06]	1.34 (B)	
2		6.87 [996]	94407 [21223]	1.86 [0.07]	1.53 (B)	
0		2.50 [363]	34355 [7723]	0.07 [0.003]	1.73 (C)	
1		5.04 [730]	69259 [15569]	1.20 [0.047]	1.63 (C)	
2		5.42 [785]	74481 [16743]	0.88 [0.034]	1.57 (C)	
0		0.49 [71]	6734 [1514]	0.04 [0.001]	3.41 (D)	
1		4.88 [708]	67060 [15075]	0.969 [0.038]	4.14 (D)	
2		5.95 [863]	81764 [18381]	1.28 [0.05]	3.57 (D)	

4.3. Effects of confinement on the slip at failure

Table 5
Average increase of bond strength and slip due to CFRP confinement.

Bar Diameter (mm) [bar #]	CFRP Layers	% Increase of bond strength	% Increase of average slip at 90% of failure pullout load
10 [#3]	0	0	0
	1	255	271
	2	283	312
13 [#4]	0	0	0
	1	222	231
	2	245	252
19 [#6]	0	0	0
	1	560	1175
	2	700	1453
25 [#8]	0	0	0
	1	567	2461
	2	680	3117

The corrosion levels, slip at 90% of failure load, and the number of layers of carbon to confine the bond specimens for 10, 13, 19, and 25 mm [#3, #4, #6, #8] bond specimens are presented in Table 5. Since the amount of slip at failure indicates the ductility of the failure mode, having a larger slip at failure would allow for redistribution of stresses reducing the brittleness at failure. For specimens confined using one layer of carbon sheet, the minimum increase in slip values was 50% compared to unconfined specimens having similar levels of corrosion. It appears that the increase in slip due to confinement is significantly higher for larger bar sizes. The slip values for 10, 13, 19, and 25 mm [#3, #4, #6, #8] specimens with respect to percent mass loss are presented in Fig. 7. Although the increase of slip at failure for 10 and 13 mm [#3 and #4] bars due to the addition of confining reinforcement was observed at high levels of corrosion, the increase never exceeded that of the unconfined bond specimens with no corrosion, even with

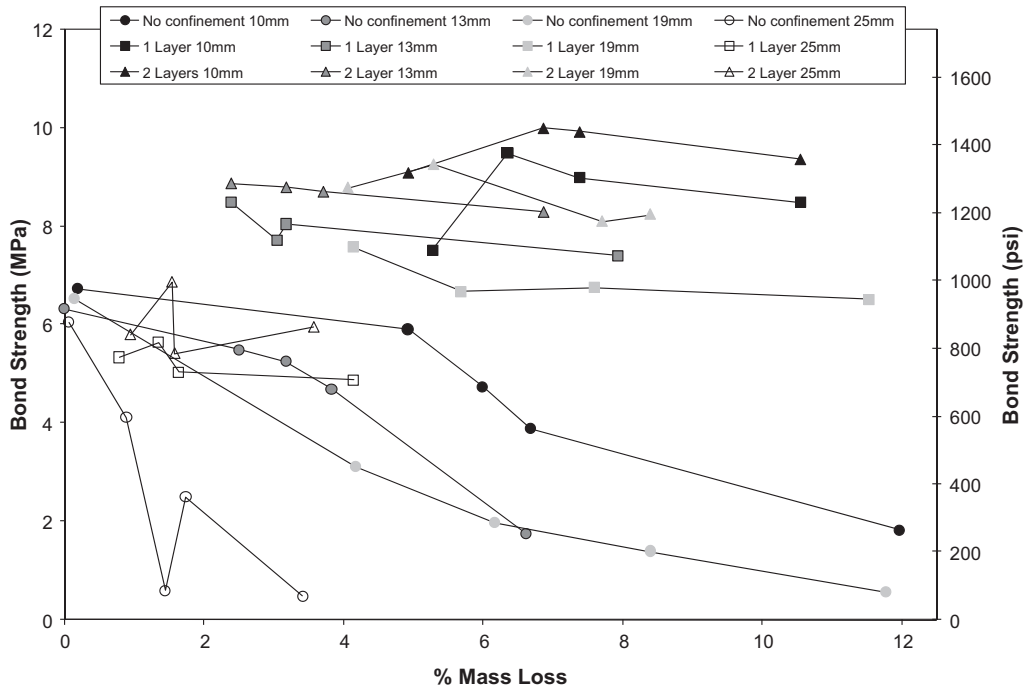


Fig. 6. Bond strength at different corrosion levels (mass loss percentages).

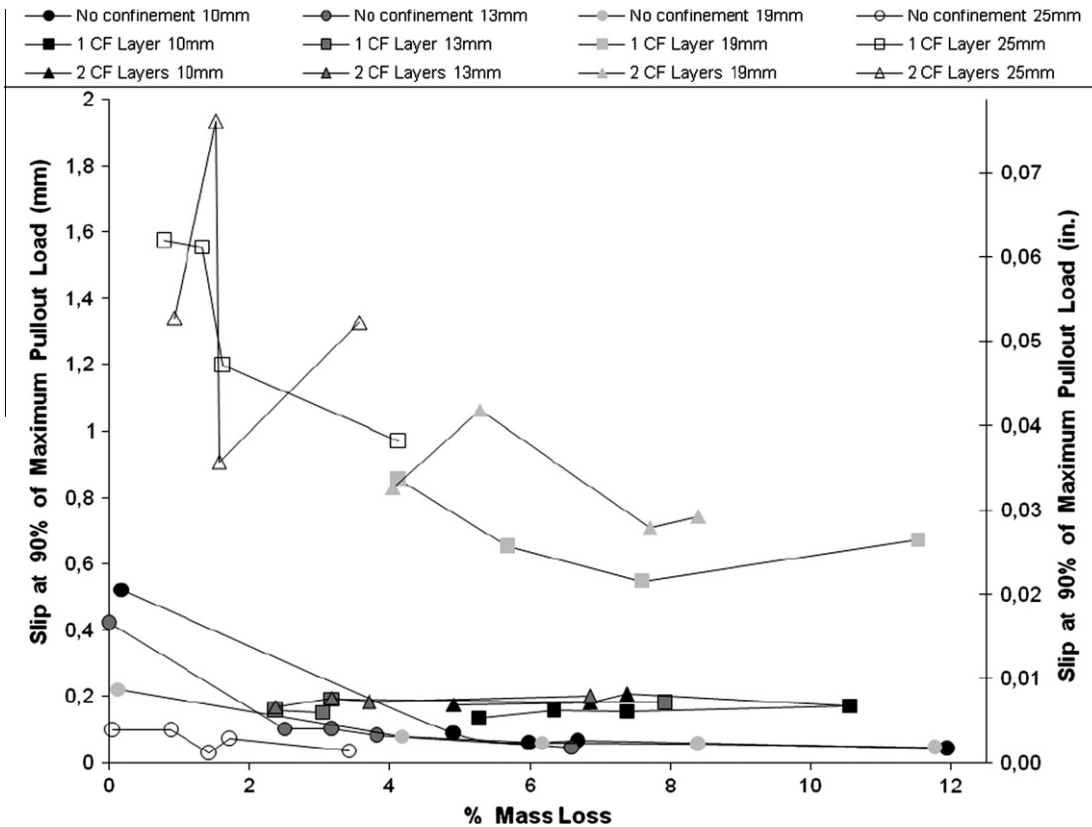


Fig. 7. Slip at different corrosion levels (mass loss percentages).

two layers of carbon sheet reinforcement. This indicates an increase of ductility for corroded structural elements in terms of bond can be achieved for 10 and 13 mm [#3 and #4] reinforcement, although not to the level of non-corroded reinforcement.

For 19 and 25 mm [#6 and #8] bars, the effect of confinement on the ductility is significant. Even with only one CFRP layer the slip is increased by 300% for 19 mm [#6] bars compared to unconfined specimens having the same amount of corrosion. An average

increase in slip at failure for non-corroded unconfined specimens was observed. This indicates that substantial increase of ductility over unconfined reinforcement is achievable for 19 and 25 mm [#6 and #8] reinforcement by providing confinement. Moreover, it was observed that the slippage of reinforcing bars is more stable for confined specimens.

4.4. Effects of confinement on the bond–slip behavior

The bond–slip behavior of specimens with 10, 13, 19, and 25 mm [#3, #4, #6, #8] reinforcing bars obtained from the pull-out

tests are shown in Figs. 8–11 respectively. For each type of confinement and rebar diameter three corrosion levels are considered (low, medium and high). The thicker lines indicate the performance of specimens confined using two layers of CFRP. Curves from the non-confined specimens are not shown in the figures. The main reason is that the curves exhibited only linear parts that coincide with the initial linear parts of curves recorded from the confined specimens. The initial linear bond–slip behavior was similar for specimens with similar amount of corrosion regardless of the CFRP layers used for confinement. In most cases, the initial linear behavior extends the longest for specimens confined by two

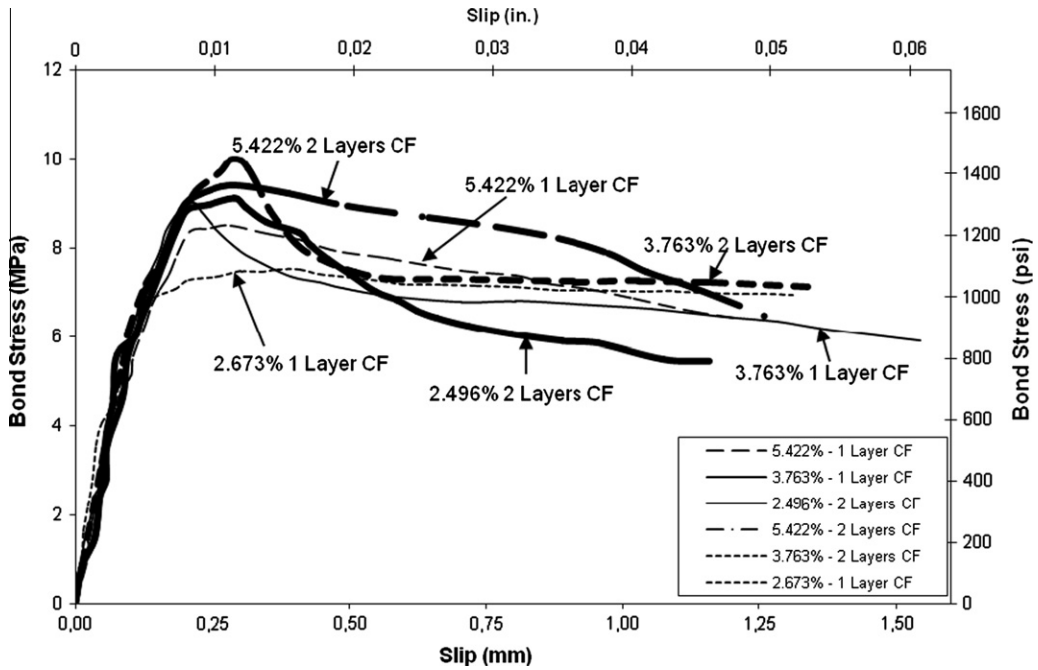


Fig. 8. Bond stress versus slip for 10 mm [#3] specimens for different corrosion levels (mass loss percentages).

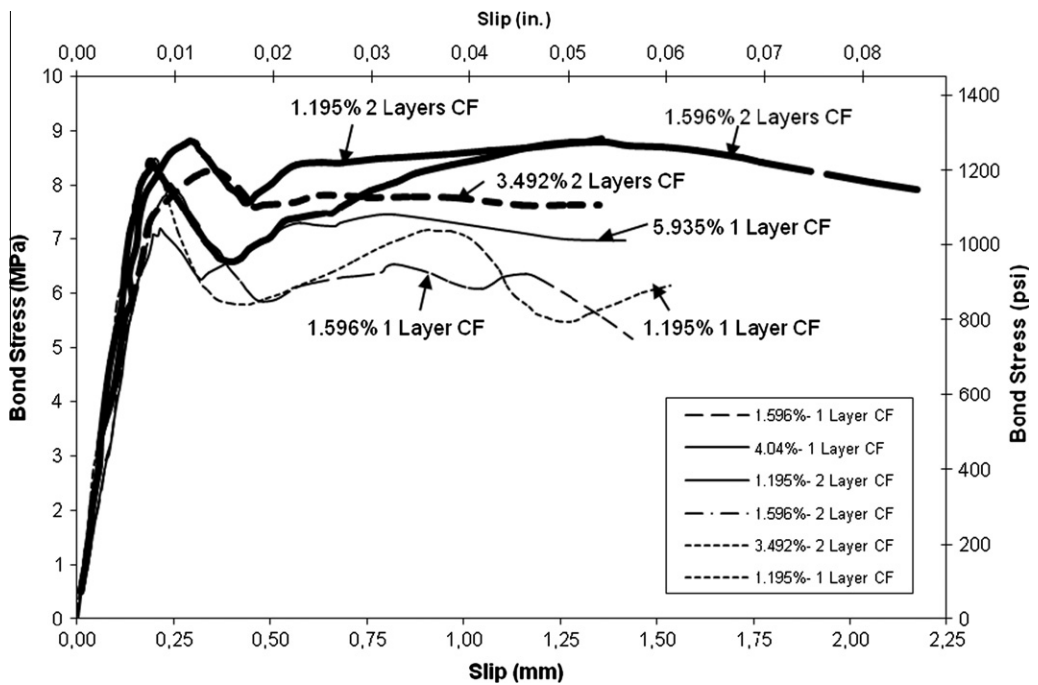


Fig. 9. Bond stress versus slip for 13 mm [#4] specimens for different corrosion levels (mass loss percentages).

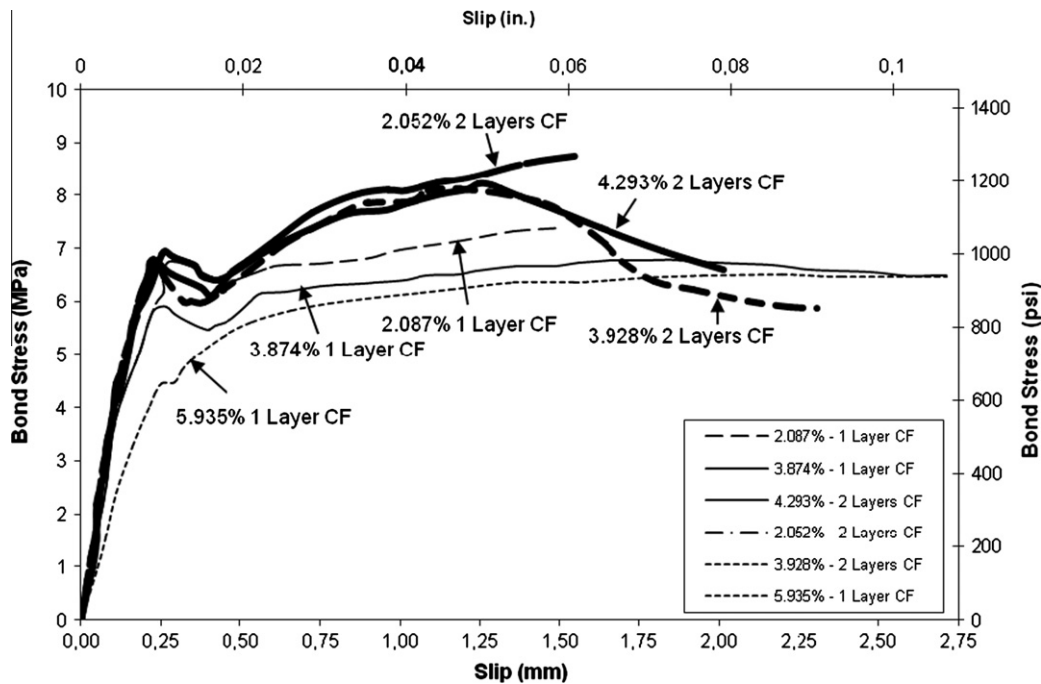


Fig. 10. Bond stress versus slip for 19 mm [#6] specimens for different corrosion levels (mass loss percentages).

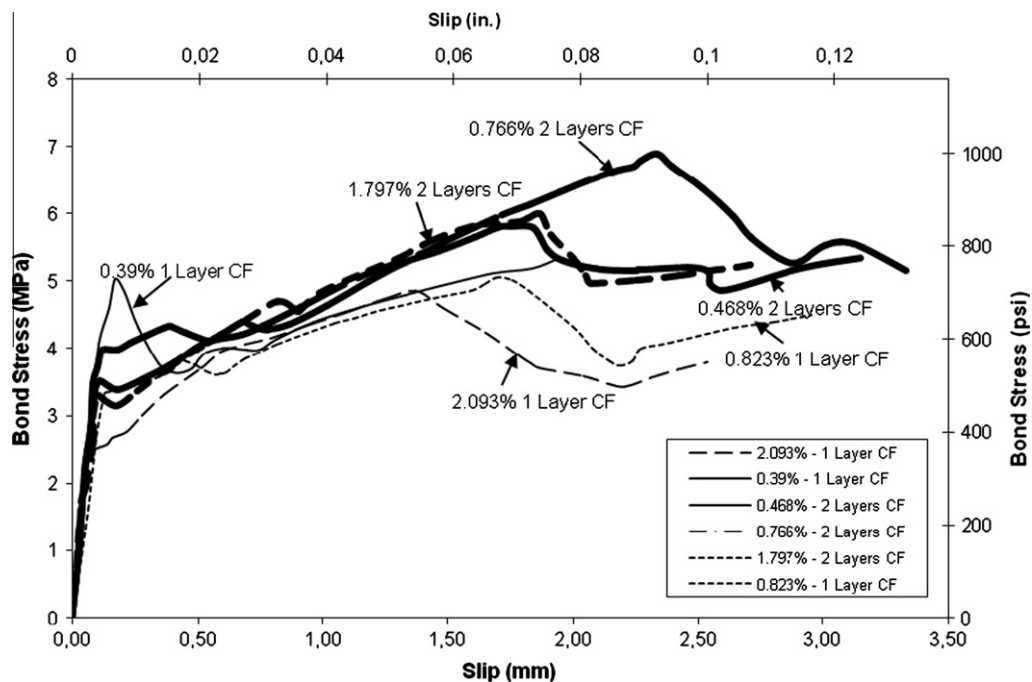


Fig. 11. Bond stress versus slip for 25 mm [#8] specimens for different corrosion levels (mass loss percentages).

layers of carbon sheet. The bond–slip behavior of confined specimens after the initial linear behavior becomes somewhat erratic as the concrete starts to fail due to the bearing of the reinforcement's ribs on the surrounding concrete. However, for most of specimens confined with two layers of carbon, the post-linear bond stress for a given slip value was higher than that of specimens confined with one layer of carbon. For 10 and 13 mm [#3 and #4] specimens, the maximum bond strengths usually occur shortly after the linear behavior. This behavior is caused by the relatively small rib area for 10 and 13 mm [#3 and #4] bars, exerting less stress on the surrounding concrete and decreasing the effects of

the confining reinforcement. For 19 and 25 mm [#6 and #8] specimens, bond stresses continued to increase in the post-linear region. Since the rib areas for 19 and 25 mm [#6 and #8] bars are relatively large, the confining reinforcement has a large effect on the pullout load.

For specimens with larger amounts of corrosion, the bond–slip behavior after the linear region is more gradual as compared to less corroded specimens. This is explained by the reduction in relative rib area as corrosion increases. The smaller ribs result in lower mechanical interlock forces and therefore the role of the confinement becomes more significant. It was observed, after the bars

were cleaned, that the rib areas (projection of rib areas normal to bar axis) were significantly reduced. As mentioned before, the role of the ribs on bond behavior is less prominent for 10 and 13 mm [#3 and #4] bars than 19 and 25 mm [#6 and #8] bars, so this gradual bond–slip behavior is also more pronounced for 19 and 25 mm [#6 and #8] bars.

5. Conclusions

The results presented in this study pertain to the bond behavior of corroded reinforcement confined by carbon fiber reinforcement. The purpose of this research is to simulate the effects of corrosion on bond behavior of confined reinforcements leading to a better understanding of confined structural elements (either using stirrups or FRP wraps). The information presented in this paper provides an insight into the contribution of confinement to bond behavior of corroded reinforcement with different diameters. Based on the results obtained and the observations made during pull-out testing of specimens, the following major conclusions can be drawn:

- The magnitude of corrosion has insignificant effect on the lateral stress (lateral to the direction that the pullout load was applied) in the confining carbon composite for small diameter bars. For larger bars, with larger relative rib areas, as corrosion increases the CFRP wrap is stressed less.
- Although at 50% of the ultimate pullout load, only a minimal amount of stress was observed in the carbon composite, at 95% of the ultimate pullout load, the amount of stress on the carbon composite increases linearly towards the free end of the corroded reinforcement. This behavior was observed in specimens with bars having larger relative rib areas.
- The percentage increase of bond strength of confined specimens, as compared to unconfined specimens, increases as the reinforcement diameter increases, due to the increase in relative rib area (19 and 25 mm [#6 and #8]).
- The percentage increase in slip at 90% of failure load for confined specimens when compared to specimens without confinement and without any corrosion is relatively small for 10 and 13 mm [#3 and #4] reinforcement but substantial for 19 and 25 mm [#6 and #8] bars.
- Although confinement does improve the behavior of corroded specimens, relative rib areas play a very important role in how effective the confinement is.
- The degradation of bond strength as the amount of corrosion increases is very small for confined specimens, even at the highest levels of corrosion (12%) that were considered.
- The bond strength obtained for specimens confined with two layers of carbon fibers is slightly higher than that of specimens confined with one layer.
- Specimens reinforced with two layers of carbon sheets were able to resist higher pullout loads than those reinforced with one layer of carbon sheet after the peak bond stress was reached.

All previous points suggest that wrapping reinforced concrete structural elements with FRP's increases bond strength, reduces corrosion-related bond slippage and hence, could provide a viable approach to deal with rebar corrosion. Several other parameters that are known to affect the bond–slip behavior of corroded steel bars should be evaluated in future studies, such as the bar cover, the quality of the concrete, the use of admixtures, and the type/coating of the bars.

References

- [1] Auyeung Y, Balaguru P, Chung L. Bond behavior of corroded reinforcement bars. *ACI Mater J* 2000;97(2):214–20.
- [2] Fu X, Chung DDL. Effects of water–cement ratio, curing age, silica fume, polymer admixtures, steel surface treatments, and corrosion on bond between concrete and steel reinforcing bars. *ACI Mater J* 1998;95(6):725–34.
- [3] Mohammed TU, Hamada H. Corrosion of steel bars in concrete with various steel surface conditions. *ACI Mater J* 2006;103(4):233–42.
- [4] Mozer JD, Bianchini AC, Kesler CE. Corrosion of reinforcing bars in concrete. *Am Conc Inst J* 1965;62(8):909–31.
- [5] Stanish K, Hooton RD, Pantazopoulou SJ. Corrosion effects on bond strength in reinforced concrete. *ACI Struct J* 1999;96(6):915–21.
- [6] Cairns J, Abdullah RB. Influence of rib geometry on strength of epoxy-coated reinforcement. *ACI Struct J* 1995;92(1):23–7.
- [7] Banic D, Grandic D, Bjegovic D. Bond characteristics of corroding reinforcement in concrete beams. Dundee, Scotland, United Kingdom: Thomas Telford Services Ltd, London, E14 4JD, United Kingdom; 2005. p. 203–10.
- [8] Al-Sulaimani GJ, Kaleemullah M, Basunbul IA, Rasheeduzzafar J. Influence of corrosion and cracking on bond behavior and strength of reinforced concrete members. *ACI Struct J (Am Conc Inst)* 1990;87(2):220–31.
- [9] Du YG, Clark LA, Chan AHC. Effect of corrosion on ductility of reinforcing bars. *Mag Conc Res* 2005;57(7):407–19.
- [10] Fang C, Lundgren K, Plos M, Gylltoft K. Bond behaviour of corroded reinforcing steel bars in concrete. *Cem Conc Res* 2006;36(10):1931–8.
- [11] Lee HS, Kage T, Noguchi T, Tomosawa F. An experimental study on the retrofitting effects of reinforced concrete columns damaged by rebar corrosion strengthened with carbon fiber sheets. *Cem Conc Res* 2003;33(4):563–70.
- [12] Tastani SP, Pantazopoulou SJ. Experimental evaluation of FRP jackets in upgrading RC corroded columns with substandard detailing. *Eng Struct* 2004;26(6):817–29.
- [13] Mangat PS, Elgarf MS. Flexural strength of concrete beams with corroding reinforcement. *ACI Struct J* 1999;96(1):149–58.
- [14] Soudki K, Sherwood T. Bond behavior of corroded steel reinforcement in concrete wrapped with carbon fiber reinforced polymer sheets. *J Mater Civil Eng* 2003;15(4):358–70.
- [15] Capozucca R, Cerri MN. Identification of damage in reinforced concrete beams subjected to corrosion. *ACI Struct J* 2000;97(6):902–9.
- [16] Kono S, Inazumi M, Kaku T. Evaluation of confining effects of CFRP sheets on reinforced concrete members. In: 2nd International conference on composites in infrastructure, Tucson, Arizona, USA. 1998. p. 343–55.
- [17] Craig BC, Soudki KA. Post-repair performance of corroded bond critical RC beams repaired with CFRP. *ACI Special Publication SP-230-33*, 2005. p. 563–78.
- [18] Soretz S, Holzbein H. Influence of rib dimensions of reinforcing bars on bond and bendability. Symposium on interaction between steel and concrete at the American concrete institute (ACI) annual convention. *J Am Conc Inst* 1978;76(1):978 [March 13–18, 1977].
- [19] Darwin D, Graham EK. Effect of deformation height and spacing on bond strength of reinforcing bars. *ACI Mater J* 1993;90(6):646–57.
- [20] Danish Standards. Pull-out test (DS 2082). Danish standards copenhagen, Denmark: Danish Standards Organization; 1980. p. 2.
- [21] ACI 318-05 Building Code Requirements for Structural Concrete and Commentary. 2005 ed., American Concrete Institute; 2005.
- [22] Fang C, Lundgren K, Chen L, Zhu C. Corrosion influence on bond in reinforced concrete. *Cem Conc Res* 2004;34(11):2159–67.